# Coexistence of strong pairing correlations and itinerant ferromagnetism arising from spin asymmetric bandwidths: A reduced BCS model study

Zu-Jian Ying,[1,2,3] Mario Cuoco,[2,3] Canio Noce,[2,3] and Huan-Qiang Zhou[1]
[1]*Centre for Modern Physics, Chongqing University, Chongqing 400044, People's Republic of China*
[2]*Laboratorio Regionale SuperMat, CNR-INFM, Baronissi, I-84081, Italy*
[3]*Dipartimento di Fisica "E. R. Caianiello", Università di Salerno, Baronissi, I-84081, Italy*
(Received 2 July 2008; published 23 September 2008)

We investigate the conditions for the occurrence of the coexisting phases that exhibit singlet superconductivity and itinerant ferromagnetism arising from spin asymmetric bandwidths. The exact solution for a reduced BCS pairing model with spin dependent bandwidths is used to determine the ground-state diagram as a function of the coupling parameter, the total density, and the topology of the single-particle spectrum. A spin-polarized superconducting state is obtained in the regime of large pair couplings with a strong bandwidth asymmetry. The analysis reveals that, for such a type of ferromagnetism, small (large) values of the density of states at energies close to the edges of the band enhance (hinder) the tendency toward a coexistence of strong pairing correlations and finite spin polarizations.

DOI: 10.1103/PhysRevB.78.104523 PACS number(s): 74.20.Fg, 75.75.+a

## I. INTRODUCTION

Superconductivity or superfluidity occurs due to some sort of attraction for quasiparticles responsible for pair formation. When pair condensation enters into competition with an intrinsic or induced source of depairing, ground-state quantum configurations can be very different from the conventional coherent states associated with a pure superconducting (SC) or superfluid phase. The search for novel quantum states, in the presence of competition between pairing and ferromagnetism, or population imbalance is nowadays at the heart of an intense research activity within apparently disparate areas, such as solid-state physics,[1] dense nuclear matter,[2–4] and ultracold trapped Fermi atoms.[5]

The nature and the stability of a coexisting phase for superconductivity and ferromagnetism strongly depend on the mechanisms that generate the spin energy mismatch and the pairing structure. For a conventional *s*-wave superconductor, early investigation pointed the attention to a type of systems where the spin imbalance is due to ferromagnetic (FM) correlations between localized magnetic impurities.[6–8] Here, the interplay of superconductivity and impurity ferromagnetism results in a configuration with an inhomogeneous spatial distribution of the spin density, either giving rise to a modulated spin structure, the so-called cryptoferromagnetism,[9] or to a ferromagnetic spiral phase.[10] In another context, inhomogeneous pairing configurations may occur for a spin imbalance induced by the Zeeman effect in an external field. In the so-called Fulde-Ferrell-Larkin-Ovchinnikov (FFLO) state, the stability of the superconducting phase is possible beyond the Clogston limit[11,12] via a modulation in the phase or in the amplitude of the order parameter.[13,14] Since its proposal, there have been a surge of activities in the search for exotic FFLO-type phases in heavy-fermion materials,[15,16] quark matter,[2] and ultracold polarized superfluids.[17–19]

If spin polarizations are due to intrinsic ferromagnetic correlations, then the coexistence of superconductivity and ferromagnetism turns out to be more difficult to survive. Nevertheless, the experimental observation indicates the itinerant ferromagnetism as a possible candidate for a thermodynamically stable state coexisting with superconductivity. This is, for example, the case for the recently discovered family of rutheno-cuprate oxides whose ferromagnetic RuO planes are separated by superconducting CuO blocks.[20] Here, the ferromagnetic/superconducting quantum states form a natural nanoscale multilayered structure including intrinsic spin and charge channels between them. Difficulties in the fabrication of single phase crystals prevent from an exhaustive comprehension of how two collective orders adjust themselves within such a system.

It has been widely accepted that the exchange of magnetic fluctuations between electrons can induce superconductivity in both the paramagnetic and ferromagnetic phases of metals.[21] Since magnetic fluctuations become large near continuous magnetic phase transitions, ideal candidates for this phenomenon seem to be itinerant ferromagnets with a low Curie temperature. In contrast to a much more common phonon-exchange coupling, which usually leads to spin singlet *s*-wave superconductivity, the magnetically mediated pairing is believed to be the strongest in the triplet *p*-wave channel. The general idea to look around a quantum critical point for magnetically mediated superconductivity has driven the discovery of a novel state of matters where collective orders, which in principle are considered as antagonists, occur together. Indeed, this is the case for heavy-fermion systems such as $UGe_2$, URhGe, UCoGe, and possibly $ZrZn_2$.[22–28]

A noticeable feature in these ferromagnetic superconductors is that the same electrons are responsible for both ferromagnetism and superconductivity in contrast to the coexistence with ferromagnetism resulted from magnetic impurities. This has renewed the interest in the long-standing problem of phase coexistence for singlet superconductivity and ferromagnetism and stimulated the search for new theoretical models to get deeper insights into possible coexistences. A BCS-type model of *s*-wave pairing, combined with a simple Stoner-type model of ferromagnetism, was used to yield a state with singlet superconductivity coexisting with ferro-

 

magnetism within mean-field approximation.[29] In this case, a careful analysis yields that the coexisting configuration is a metastable state with respect to the nonmagnetic superconducting state or the normal ferromagnetic one.[30–33]

A theoretical analysis in the context of exact solution shows that the coexistence of pairing correlations and spin polarizations may lie in mesoscopic systems such as metallic grains.[34–36] A model of BCS-type pairing and Stoner exchange interaction, known as the universal Hamiltonian, has been introduced to describe the low-energy physics of small metallic grains in the diffusive limit, with a large Thouless energy compared with the single-particle mean-level spacing.[37,38] In such a finite-size system, according to the strengths of the pair coupling and the magnetic exchange, there occurs a small window around the Stoner threshold where the ground state is a paired state with a finite spin polarization.[34] This parameter regime with the coexistence of pairing correlations and a partial spin polarization may be enhanced by applying an external magnetic field[39] by introducing mesoscopic fluctuations[40] or by switching on asymmetric spin dependent bandwidths in the single-particle spectrum.[34] For grain systems, it should be noticed that the coexistence of ferromagnetism and superconductivity has been recently observed in Sn nanoparticles.[41]

It is worth mentioning that a weakened depairing strength makes easier for the ferromagnetic order to compromise with the superconducting correlations. One may search for different microscopic mechanisms that lead to the itinerant ferromagnetism.[42] Another way to soften the depairing effects to form a coexistence of strong pairing correlations and spin polarizations is provided by the inclusion of an antiferromagnetic spin-exchange coupling,[35] which may also be intrinsically manifest in superconducting grains.[37] In such a case, the topological manipulation of the polarized and pair spectrum via filling control and size variation can give rise to quantum configurations with robust pairing correlations even in the presence of a large magnetization.[36]

In this paper, we propose another route to stabilize a coexisting superconducting-ferromagnetic phase in a mesoscopic or bulk system by choosing proper types of the single-particle density of states (DOS) and tuning the total particle density, with ferromagnetic correlations induced by spin dependent bandwidths. The analysis is focused on possible inhomogeneous configurations in the energy space that may allow the coexistence of strongly paired and ferromagnetic polarized configurations. A key aspect in such a scenario is the energy profile of the single-particle spectrum with an effective pairing. We show that the level distribution in the energy space plays a significant role in stabilizing quantum configurations with *strong* pairing correlations and nonzero spin polarizations. We demonstrate that the transition from a nonmagnetic state to a spin-polarized paired state can be tuned from first order to second order if pairing amplitude is varied from weak to strong coupling. The analysis is based on the comparison between the ground-state diagram of model systems with different spectrum topologies resulted from dimensionality or intrinsic inhomogeneous DOS. For the type of ferromagnetism examined, the coexistence is strengthened (weakened) if the DOS is smaller (larger) at the edges of the band when compared to the values of the DOS at the band center. The mechanisms related with the coexistence are analyzed in detail so as to yield a general perspective as far as the realization of quantum paired ground state with nonzero spin polarization is concerned.

The paper is organized as follows. In Sec. II we present the model Hamiltonian, together with its symmetry properties, and sketch the exact solution of the model, briefly examining the role played by the number of single-particle energy levels. Section III refers to the study of the ground-state diagram with the pair coupling and the asymmetry ratio of the spin bandwidths as control parameters for a uniform DOS. In particular, we carefully analyze the mechanisms related to the occurrence of weakly and strongly paired coexisting phases. Then, we discuss the effects induced by different topologies of the single-particle spectrum in Sec. IV, addressing the DOS for systems in one, two, and three dimensions. Finally, Sec. V is devoted to the concluding remarks.

## II. MODEL: SYMMETRY PROPERTIES AND EXACT SOLUTION

We consider a BCS pairing Hamiltonian with a discrete single-particle spectrum,

$$H = \sum_{j=1}^{\Omega} \sum_{\sigma=+,-} w_\sigma \varepsilon_j \hat{n}_{j\sigma} - g \sum_{j,j'} c_{j+}^\dagger c_{j-}^\dagger c_{j'-} c_{j'+}. \tag{1}$$

Here, $w_\sigma$ is the parameter that controls the spin bandwidth amplitude and $g$ is the strength of the pair coupling between two particles within the same level with opposite quantum numbers $(+,-)$ associated with the spin polarization, and $\Omega$ is the total number of levels. The first term of Hamiltonian (1) indicates the single-particle energy contribution with a spin asymmetric spectrum, while the second part involves a conventional BCS-type pairing interaction with zero total momentum. The symmetric-band case is known as the reduced BCS model or the Richardson pairing model, which has been widely used in nuclear physics,[43] mesoscopic physics,[38,44,45] and trapped cold atoms.[46] The spin dependent bandwidths may have different origins. In solid-state physics, the Coulomb interaction can drive a ferromagnetic instability with a gain in the kinetic energy,[47] thus leading to a difference between the effective masses of the majority and minority carriers. In complex oxides, a similar effect is induced by the interplay of orbital and spin degrees of freedom via the so-called double exchange mechanism.[48,49] If one considers ultracold Fermi gas, the asymmetry is readily introduced by a mixture of atoms with unequal masses.[3,50–52] In the present paper we focus on the interplay of pairing and depairing effects while keeping in mind their relevance to the coexistence of superconductivity and ferromagnetism. The strategy we follow is to get a basic understanding of the competition between superconducting and ferromagnetic correlations by analyzing the mechanisms that control the system properties for a uniformly distributed spectrum $\varepsilon_j = -(\Omega+1-2j)d/2$, $j=1,\ldots,\Omega$. Then, we concentrate on the role played by an energy-dependent DOS with a structure that refers to a tight-binding spectrum for one-, two-, or

three-dimensional lattices with a dispersion $\varepsilon_{\vec{k}}=-D/(2r)\Sigma_i \cos k_i$, where $i$ sums over the directions $x$, $\{x,y\}$, or $\{x,y,z\}$ and $r=1$, 2, or 3 for different dimensions, respectively. Let $d$ denote the mean-level spacing while $D=\Omega d$ yields the amplitude of the bandwidth. For convenience, we introduce the bandwidth ratio $\omega=w_-/w_+$ to measure the strength of the spin asymmetry, while the pair level spacing $2d$ is taken as the scale unit of energy with a consequent constraint $w_++w_-=2$.

### A. Particle-hole symmetry

The Hamiltonian presents a symmetry property that allows us to reduce the computational cost. Indeed, when considering a symmetric dispersion with respect to the center of the energy band $\varepsilon_c$, as $\varepsilon_j-\varepsilon_c=-(\varepsilon_{\Omega-j+1}-\varepsilon_c)$, the model Hamiltonian exhibits a particle-hole symmetry. Such cases include both the uniform DOS and nonuniform spectrum with the dispersion in the form of a cosine function of the momenta in one, two, or three dimensions. As the reference energy, the band center can be simply set to be the zero energy point, i.e., $\varepsilon_c=0$. The particle-hole transformation,

$$c_{j\sigma}\rightarrow \bar{c}^{\dagger}_{j\sigma}, \quad \hat{n}_{j\sigma}\rightarrow 1-\hat{\bar{n}}_{j\sigma},$$

renders Hamiltonian (1) to the form

$$H=\sum_{j,\sigma} w_\sigma \varepsilon_j \hat{\bar{n}}_{j\sigma}-g\sum_{j,j'} \bar{c}^{\dagger}_{j'-}\bar{c}^{\dagger}_{j'+}\bar{c}_{j+}\bar{c}_{j-}+C, \tag{2}$$

where $C=\Sigma_j\Sigma_\sigma w_\sigma\varepsilon_j+[g(\Omega-N)]$ is a constant term in the canonical ensemble for a given total particle number $N$. As one sees, the Hamiltonian keeps the same form either in terms of the particle creation and annihilation operators ($c^{\dagger}_{j\sigma}$ and $c_{j\sigma}$) or in terms of hole operators ($\bar{c}^{\dagger}_{j\sigma}$ and $\bar{c}_{j\sigma}$) up to an irrelevant constant. Therefore, one only needs to limit the analysis at densities below the half filling $\rho\equiv N/(2\Omega)=0.5$ since the case above is readily obtained by exploiting the particle-hole symmetry consideration.

### B. Exact solution

In this section, we briefly sketch the exact solution of the quantum pairing problem. Hamiltonian (1) is exactly solvable both for symmetric[43,53] and asymmetric spectra.[34] According to the Pauli principle, singly occupied levels are blocked from the pairing scattering. In the presence of $N_p$ pairs over the unblocked levels $\Omega_U$ with the remaining $N-2N_p$ single particles in the blocked sector $\Omega_B$, the dynamics of the system is composed of a pairing part and an unpaired one, which are decoupled from each other. Based on such an observation, one can show that a generic eigenstate of $H$ is expressed as a product state $\Psi=\Psi_B\otimes\Psi_U$, where $\Psi_B=\Pi_{j\in\Omega_B}c^{\dagger}_{j\sigma_j}|0\rangle$ and $\Psi_U=\Pi_{\mu=1}^{N_p}\Sigma_{j\in\Omega_U}\frac{c^{\dagger}_{j+}c^{\dagger}_{j-}}{(w_++w_-)\epsilon_j-E_\mu}|0\rangle$. The corresponding eigenenergy sums up the contributions from the two parts,

$$E=\sum_{\mu=1}^{N_p} E_\mu+\sum_{\sigma,j\in\Omega_B} w_\sigma\epsilon_j. \tag{3}$$

The pair energy $E_\mu$ is determined from the Richardson equations,[43]

$$\frac{1}{g}+\sum_{\nu=1(\nu\neq\mu)}^{N_p}\frac{2}{E_\nu-E_\mu}=\sum_{j\in\Omega_U}\frac{1}{(w_++w_-)\epsilon_j-E_\mu}. \tag{4}$$

In order to accommodate a fully paired, i.e., an unpolarized phase, we consider an even total number of particles $N$ given by $N=2M$, with $M$ being the maximum total number of pairs.

### C. Role of the total number of levels: Crossover from mesoscopics to macroscopics

Before presenting the results for the ground-state diagram, we address the effects induced by varying the total number of levels. One notices that the ground-state energy can be analytically handled in a specific range of parameters to estimate the role of the total number of the single-particle levels. Given a set of $2m$ blocked levels and $\Omega-2m$ unblocked ones, the pairing energy of the ground state can be obtained by performing a strong-coupling expansion in $1/g$,[54]

$$E_m^U\approx -(M-m)(\Omega-M-m+1)g+s_1\frac{M-m}{\Omega-2m}-\left(s_2-\frac{s_1^2}{\Omega-2m}\right)\frac{(M-m)(\Omega-M-m)}{(\Omega-2m)^2(\Omega-2m-1)g}, \tag{5}$$

where $s_p=\Sigma_{j\in\Omega_U}[(w_++w_-)\varepsilon_j]^p$. Note that we have taken into account the level blocking from polarized particles. To facilitate our mechanism analysis in the Sections III C–III E, only the expansion up to the $1/g$ order has been kept. Equation (5) gives a good approximation for values of $\lambda$ within a range of $\sim[0.75,\infty]$,[35,36] with $\lambda=g\Omega/D=g/d$ being the average relative pairing strength. Still, the convergence of higher-order expansions can be extended up to $\lambda\approx 1/\pi$.[54]

Numerically, we have checked the ground-state diagram for different values of the total number of levels $\Omega=100,200,300,\cdots$. It is found that, at a given total particle density $\rho$, the increase in the total level number does not cause any qualitative change to the phase diagram in ($\lambda$-$\omega$) plane. Such an observation can be understood as follows. In the leading order of the expansion, after averaging over the unbroken $M-m$ pairs and neglecting a small term of the order of $1/\Omega$, we find that the pairing energy $E_m^U/(M-m)/D\sim-[1-\rho(1+P)]\lambda$ is independent of the total level number $\Omega$. Here $P=m/M$ is the pair breaking rate and the energy is rescaled by the bandwidth amplitude $D$ in accordance with the competing single-particle energy $w_\sigma\varepsilon/D$ for polarized configurations, which also shows no significant changes as a function of the total number of levels. A similar argument also applies to higher orders in the expansion. In fact, the averaged pairing energy in the expansion is a function of the relative pairing strength $\lambda$, the density $\rho$, the pair breaking rate $P$, and the rescaled spectrum polynomial $s_p$,

$$\frac{E_m^U}{(M-m)D}=F\left[\lambda,\rho,P,\frac{s_p}{D^p\Omega}\right]+o\left(\frac{1}{\Omega}\right). \tag{6}$$

The $1/\Omega$ correction becomes negligible for $\Omega\geq 100$. The other effects due to a variation in the level number appear in the spectrum polynomial which approaches a constant integral value,

$$\frac{s_p}{D^p\Omega} = \frac{1}{\Omega}\sum_{j\in\Omega_U}\left[\frac{2\varepsilon_j}{D}\right]^p \to \int_{-1/2}^{1/2}(2\epsilon)^p \varrho_U(\epsilon)d\epsilon.$$

Here, $\varrho_U$ is the DOS for the pairing unblocked part. Then, the increase in the level number gives rise to a variation that is about the difference between the value of the integral and the result of the summation over the energy levels. Still, this change is insignificant as far as the qualitative features of the ground state are concerned.

The above discussion demonstrates that different level numbers bring to the same ground-state diagram qualitatively, with comparable values of the critical spin band asymmetry ratio at a given pairing strength λ and an assigned filling $\rho$. It is worth pointing out that, for mesoscopic systems, the reduction in the size generally influences the level number as well as the level spacing. In this case, a careful analysis is required to consider the variation for λ induced by the size change.[36,55–57]

## III. COMPETITION BETWEEN STRONG PAIRING CORRELATIONS AND SPIN POLARIZATIONS: A CONSTANT DOS

### A. Ground-state diagram: Occurrence of a strongly paired configuration with partial spin polarizations

At a given total density away from the half filling, the mismatch between the Fermi levels of the two spin bands, due to the bandwidth asymmetry, tends to induce a finite magnetization. On the other hand, the attractive pairing interaction favors the formation of pairs with zero total spin in such a way that their number is maximized. The interplay between these two tendencies leads to different ground-state configurations. We presented a detailed ground-state diagram in Fig. 1 at a given filling $\rho=0.2$ for a uniform spectrum. SC and FM stand for the superconducting ground state without polarization and the ferromagnetic state with the maximum allowed spin polarization, respectively. Moving from SC to FM, one obtains a coexisting region for paired and spin-polarized particles, where the boundaries separate the area of coexistence into subregion slices with different number of broken pairs. In the diagram one can observe two distinct regions: (i) region F with sparse boundaries, where the spin-polarized particles reside around the uncorrelated Fermi level; (ii) region B with dense boundaries, where the pair breaking occurs at the bottom of the band. Such aspects can be accounted for by inspection of the pair density distribution associated with different ground-state configurations as presented in Fig. 2.

It should be noticed that region B is characterized by strong pairing correlations that survive in the presence of finite polarizations. This is reflected in both the rapidity of boundary evolution and the pair distribution. An indication of strong pairing correlations comes from the observation that the boundaries in region B vary rapidly when the pair coupling λ increases, in a sharp contrast to their slow evolution in region F (see Fig. 1). After the initial polarization at SC/B boundary, the further polarizations in region B are still very sensitive to the change in the pair coupling. This indicates that the energy of pairing correlations is still playing a dominant role in the energy cost for breaking pairs. A more explicit evidence for the strong pairing correlations lies in the pair distribution. For states in region B, there is a more homogeneous energy distribution of the pair occupation over all the unblocked levels [see Fig. 2(b)], while for configurations in region F the pair density is completely unbalanced

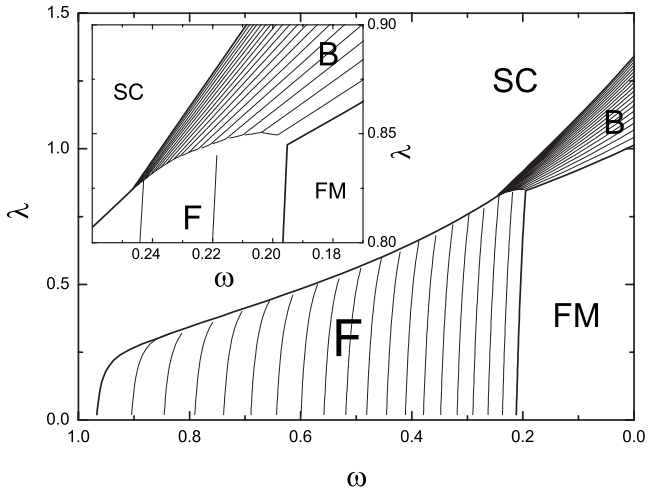


FIG. 1. Detailed ground-state diagram in the plane of the pair coupling $\lambda=g/d$ and the bandwidth ratio $\omega=w_-/w_+$ for a total density $\rho=0.2$ assuming a spectrum with 100 levels. Here, $g$ gives the pairing constant and $d$ is the mean single-particle level spacing. The bandwidth asymmetry becomes stronger (weaker) when $\omega=0$ ($\omega=1$) is approached. SC (FM) labels the superconducting region without any polarization (ferromagnetic region with a full polarization). The boundaries separate the diagram into regions with different numbers of broken pairs. The quick (slow) variation in the dense (sparse) boundaries in region B (F), with respect to the increase in pair coupling, indicates a ground state with strong (weak) pairing correlations coexisting with partial spin polarizations. The inset is an enlarged view of the region where SC, F, FM, and B get connected.

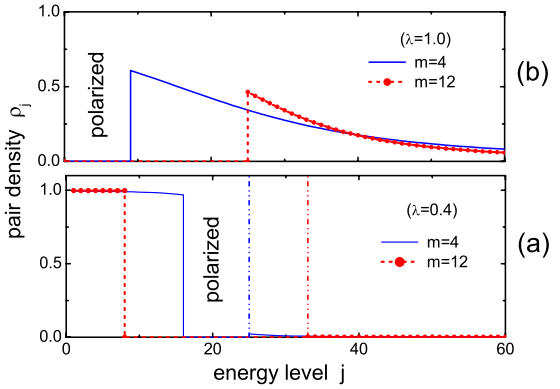


FIG. 2. (Color online) (a) and (b) represent the energy distribution of the pair density for the B- and F-type configurations at different broken-pair numbers of $m$ for $\rho=0.2$ over $\Omega=100$ levels ($j=1,\ldots,\Omega$), respectively. The uncorrelated Fermi level is located at $j=20$. The blocked sector corresponds to the energy window where the pair density is zero, with levels singly occupied by polarized particles.

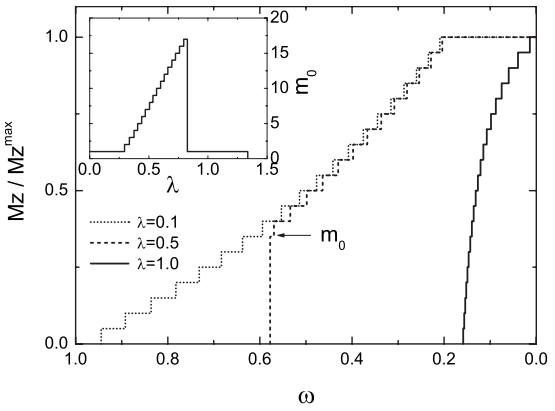


FIG. 3. Evolution of the magnetization as a function of the spin band asymmetry ratio $\omega$ at different values of the pair coupling $\lambda$ for $\rho=0.2$ and $\Omega=100$. Here $m_0$ indicates the number of broken pairs that occur at the boundary between region SC and regions with partial polarizations. In the inset, the behavior of $m_0$ is reported as a function of $\lambda$ along the boundary line of region SC.

between the unblocked part above the blocked sector and that below [see Fig. 2(a)]. This demonstrates that pairs in region B are strongly correlated, in contrast to the weak pairing correlations in region F, since stronger (weaker) pairing will induce more (less) pair hopping over all unblocked levels.

Unlike the small weight of the pair distribution above the blocked sector in region F, the strong pairing correlations in region B have resulted in a pair density that distributes completely above the blocked sector. This also leads to another feature of region B that the single-level particle density above the blocked sector can be even higher than that in the blocked sector due to the bandwidth asymmetry. In fact, as shown in case $m=4$ (solid blue line) in Fig. 2(b), the particle density $2\rho_j$ close to the blocked sector is obviously larger than that in the singly occupied blocked sector (one particle per level), i.e., $2\rho_j>1$. Here, $\rho_j$ is the pair density at a level $j$ in the single-particle spectrum. The pair density above the blocked sector varies to match a necessary condition for the ground state that the single-level energy for the pairing level, $2\rho_j\varepsilon_j$, is lower than a polarized level $w_+\varepsilon_j$ in occupation competition. This allows the possibility for the aforementioned large pair density $(2\rho_j>1)$ as $w_+>1$.

### B. Evolution of the magnetization versus the spin band asymmetry and the pair coupling: Softening of a magnetization jump

To monitor the transitions from the unpolarized SC or fully magnetized FM phase toward the coexisting regions, it is useful to analyze the behaviors of the total magnetization. The breakdown of the SC state is accompanied by different types of transitions. As one can see in Fig. 3, at filling $\rho=0.2$, for intermediate values of the pair coupling ($\lambda\sim[0.3,0.8]$), the band asymmetry induced transition is first-order-like with a jump in the magnetization (see the example of $\lambda=0.5$) at the SC/F boundary. The feature of the transition is completely modified for larger pair couplings at the SC/B boundary. The first-order transition gets softened to be second-order-like, with the magnetization increasing gradually from zero (see the example of $\lambda=1.0$). It should be noted that the softened magnetization in region B is essentially different from the weak pair coupling regime. In fact, the polarization for region B (as shown in case $\lambda=1.0$ in Fig. 3) does not show up until the strength of the band asymmetry reaches some critical point, while the case $\lambda=0.1$ in the weak-coupling regime shows that the magnetization occurs as the band asymmetry is switched on. As we shall discuss in Section III C, the former case arises from the topological change in the blocked spectrum, thus allowing the occurrence of strong pairing correlations, while, in the latter case, the absence of magnetization jumps is due to the fact that the pair coupling is much smaller than the level spacing, so it is too weak to induce considerable interlevel pairing correlations.

### C. Mechanisms for weakly and strongly paired phase coexistences

We have shown in Fig. 1 that there are two different regions F and B where pairs are partially polarized. From the exact solution, one can see that pairs are always correlated via hopping over the unblocked levels as long as the saturation magnetization is not yet reached such that there are more unblocked levels for the unpolarized pairs to occupy. In other words, a partially polarized ground state is always a coexisting state of pairing correlations and ferromagnetic order. However, the strength of pairing correlations in regions F and B differs significantly from each other, being very weak and very strong, respectively. One can readily see their difference from the weight of pair distribution over high-energy levels in Fig. 2, since stronger (weaker) pairing correlations mean that pairs distribute more (less) homogeneously over all the unblocked levels. In this section we address the mechanisms, which arise from the difference in the topology of paired and unpaired spectra, which lead to a dramatic change in pairing correlations from region F to region B.

#### *1. Reduction in the pair-correlation strength for the ground state with spin polarizations around the Fermi level*

As discussed previously, the ground state in region F is characterized by a spin polarization that develops around the uncorrelated Fermi level. In this circumstance, it is possible to show that the depairing tends to renormalize the pairing correlations as soon as a nonzero spin polarization is formed. To see this we shall analyze and compare the energy variations for the polarized and pairing parts.

The polarization of a pair is accompanied by a gain in the single-particle energy due to the spin band asymmetry. This energy gain is negative and tends to lower the total energy. Once the negative-energy gain covers the cost for breaking pairs, a polarization is induced. When the pair breaking occurs around the Fermi levels as in region F, the number $m$ of the polarized pairs fill up the singly occupied sector from the level $\varepsilon_{M-m+1}$ to $\varepsilon_{M+m}$ in the spin-up band, thus providing a blocked sector energy $E_m^B=w_+\Sigma_{j=M-m+1}^{M+2m}\varepsilon_j=-w_+m(\Omega-N)d$.

On average, for each broken pair, the energy gain becomes $E_m^B/m=-w_+(\Omega-N)d$, which is negative, as aforementioned, because there are more levels than single particles ($\Omega>N$) at a total density below the half filling. The energy gain is still negative above the half filling, since $N$ in this case becomes the hole number after the particle-hole transformation, if one adopts the above form of $E_m^B$. Here in region F, it should be noted that the average energy gain does not vary with the number of polarized pairs.

Now, we turn to the analysis of the change in the strength of pairing correlations after a spin polarization is induced. Assuming $m$ pairs are broken, then the reduction in the pairing levels leads to an energy rise, $\Delta E_m^U=E_m^U-E_0^U$, in the unblocked part. The averaged energy cost per broken pair is $\Delta E_m^U/m$, covered by the negative-energy gain in the occurrence of polarizations. Suppose that strong pairing correlations still remain after a depairing from the fully paired SC state, then the average cost for the pair breaking in the paired sector has a leading order $\Delta E_m^U/m=(E_m^U-E_0^U)/m\approx(\Omega-m+1)g+\frac{N-2m}{\Omega-2m}(\Omega-N)d$, as extracted from Eq. (5). The first term comes from the reduction in the pair hopping. The second term is due to the rise of the pair kinetic energy, since the blocked sector around the Fermi level is below the zero energy point $\varepsilon_c=0$, at a filling $\rho<0.5$, so that relatively there are more unblocked levels left for pair scattering above $\varepsilon_c$ than below $\varepsilon_c$. For a small broken-pair number $m$ and an intermediate value of $\lambda$, the factor $(\Omega-N)$ in the second term is much smaller than $(\Omega-m)$ from the first term, while for a large $m$, the other factor $\frac{N-2m}{\Omega-2m}$ also reduces the influence of the second term. Therefore, the pair hopping leading contribution ($g$ term) plays the dominant role, which decreases with increasing values of $m$. Thus, the average energy cost $\Delta E_m^U/m$ becomes smaller when more pairs get broken, while the afore discussed average energy gain $E_m^B/m$ is unaffected by varying $m$. As a result, the maximum allowed number of the broken pairs is energetically the most favorable. As long as the pairing correlations are strong, this mechanism favors the maximization of the number of the broken pairs until only weak pairing correlations are left due to the large blocking effect. Therefore, in region F, the pairing correlations are immediately renormalized down to a weak regime as soon as the spin polarization becomes different from zero.

In such weak pairing correlations, the hopping of pairs from levels below the polarized sector to the levels above it is greatly hindered due to the large blocking effect occurring to configuration F that has a blocked sector around the uncorrelated Fermi level. In this situation, intralevel couplings dominate the pairing energy. Thus, instead of the aforementioned energy form in the case of a strong coupling, configuration F with $m$ broken pairs has a leading-order total energy $E_m\approx\Sigma_{j=1}^{M-m}2\varepsilon_j-g(M-m)+\Sigma_{j=M-m+1}^{M+m}w_+\varepsilon_j$. Here, the first and third terms are single-particle energies for pairs and polarized particles, respectively. The second term is the intralevel pairing energy, while we have neglected the interlevel pairing part which contributes to higher orders.[58] The energy crossover $E_{m-1}=E_m$ gives rise to the boundary between neighbor subregions with $m-1$ and $m$ polarized pairs,

$$w_+^{m-1,m}\approx\frac{2\varepsilon_{M-m+1}-g}{\varepsilon_{M-m+1}+\varepsilon_{M+m}}=1+\frac{(2m-1)+\lambda}{\Omega-2M}. \quad (7)$$

Note that the small factor $1/(\Omega-2M)$ here renormalizes down the influence of the pair coupling $\lambda$, which accounts for the slow evolution of the boundaries in region F with respect to $\lambda$, as mentioned in Sec. III A.

#### *2. Minimization of the blocking effect and emergence of a softly polarized ground state with strongly correlated pairs*

For states in region B, the spin-polarized particles occupy the bottom of the band. The emergence of strong pairing correlations in this region is closely related to this topological feature of the blocking sector. Indeed, as we have discussed above, the presence of a blocked sector around the uncorrelated Fermi level tends to weaken the pairing correlations. The growth of the pair coupling in region B relative to region F leads to a modification of the blocking sector by shifting its position to the bottom of the band. This configuration for the spin-polarized particles minimizes the blocking effect on the paired part. Because there is a significant pair hopping for larger values of $\lambda$ as in region B, the pairs are distributed more uniformly over the unblocked levels. Hence, the effective pair density per energy level gets smaller than the single-particle one, and, as a result, there is an optimization of the single-particle energy gain by filling the lowest-energy levels with spin-polarized particles. Since there is no unpaired sector to split the pairing part, the pair hopping is not constrained at all. Thus, pairing correlations get maximized.

Besides the maximum pairing correlations, the topological character in the B configuration also brings about the softening of magnetizations, in contrast to the initial polarization jump at the boundary between regions SC and F. The spin polarization in region B is activated in an almost continuous way, in the sense that the strongly correlated pairs are broken one by one, as we have shown for $\lambda=1.0$ in Fig. 3. Moreover, strong pairing correlations are still maintained at each variation in the magnetization. In what follows, we deduce such an effect by inspection of the leading order for the total energy.

(i) *Large polarization tendency from the pairing part.* By breaking $m$ pairs from a fully paired state in region SC, the total-energy cost associated with the unblocked part is about $\Delta E_m^U\approx m(\Omega-m+1)g+m(N-2m)d$. The first term in $\Delta E_m^U$ is a consequence of the reduction in the pair hopping, the same as it occurs in region F. The second term is due to the rise of the center mass for the unblocked spectrum and it is different from its counterpart in region F due to an unequal position of the blocked sector. On average, for each broken pair, the energy increase is $\Delta E_m^U/m\approx(\Omega-m+1)\lambda d+(N-2m)d$, and it favors the largest allowed number of broken pairs because it decreases when $m$ grows, similarly to what happens in region F.

(ii) *Small polarization counteraction from the polarized part.* The energy cost for depairing is balanced by the energy gain in the blocked spin-polarized sector $E_m^B=w_+\Sigma_{j=1}^{2m}\varepsilon_j=-w_+m(\Omega-2m)d$. Here, in region B, the polarized particles from the $m$ broken pairs fill the energy levels from the lowest

$\varepsilon_1$ up to $\varepsilon_{2m}$. Note that, on average, $E_m^B/m=-w_+(\Omega-2m)d$, and thus each broken pair has a less negative energy if $m$ increases. Now, for the unpaired part, the *smallest* number of polarized pairs is energetically favorable, which counteracts with the maximum-$m$ mechanism from the correlated pairs.

(iii) *Reversion from large to small polarizations.* To reverse the tendency of a large polarization from the pairing part, the asymmetry $w_+$ should be strong enough so that not only the influence of the $m$ terms in $\Delta E_m^U/m$ is covered by the counterpart in the polarized sector but also the average energy cost of depairing is reached. The crossover between the two competing mechanisms occurs when $-E_m^B/m=\Delta E_m^U/m$, leading at the lowest order of pairing strength to the crossover from the SC state to the $m$-broken-pair configuration, $\lambda_m \approx \lambda_m^0=\frac{w_+(\Omega-2m)-2(M-m)}{\Omega-m+1}$, while a higher-order analysis including the $1/\lambda$ term in Eq. (5) yields $\lambda_m \approx \lambda_m^1=\lambda_m^0/2+\sqrt{(\lambda_m^0/2)^2-1/3}$ after dropping the $1/\Omega$ terms. The one-by-one pair polarization requires that $\lambda_m$ is larger for less broken pairs (otherwise the energy crossover for more pair breaking occurs earlier with a polarization jump). One can show that this condition is fulfilled when $w_+$ $(\omega=w_-/w_+)$ is larger (smaller) than a critical value for the spin asymmetry ratio. Let us denote this critical point by $\omega_B^c$. Correspondingly the pair coupling is stronger than a critical value $\lambda_B^c$. Then, for $\omega<\omega_B^c$ and $\lambda>\lambda_B^c$, the spin polarization in regime B is driven by a one-by-one pair breaking. The critical values $\omega_B^c$ and $\lambda_B^c$ can be extracted from solving the equation $\partial\lambda_m/\partial m=0$, which gives rise to

$$\omega_B^c \approx \rho/(1-\rho),$$

$$\lambda_B^c \approx (1-2\rho)+\sqrt{(1-2\rho)^2-1/3}, \tag{8}$$

at the leading order. These expressions are valid for $\rho \leq \rho_{FB}$, where regions F and B are disconnected, with $\rho_{FB}$ being determined by Eq. (11) below. For the filling $\rho=0.1$, the location of $\omega_B^c$ is marked in Fig. 4. For $\omega>\omega_B^c$ and $\lambda<\lambda_B^c$, breaking more pairs becomes favorable, leading either to a direct transition from the SC phase to the FM phase or to an intermediate polarization jump in entering region F (see Fig. 4 at a given filling $\rho=0.1$).

(iv) *Strong pairing correlations maintained in growing polarizations inside region B.* The above analysis shows the softened initial polarization at SC/B boundary. Deeper into region B, with more broken pairs, it is still favorable for the ground state to remain in the same topological structure of the unpaired spectrum. When the polarization grows, the total pair density $\rho_U=(M-m)/(\Omega-2m)$ over the remaining $\Omega-2m$ unblocked levels becomes more dilute at a filling below the half. Generally, the decrease in the total pair density also reduces the local pair density $\rho_j$ on each level. Then, the pairs with an energy $2\rho_j\varepsilon_j$ for a single level $j$ get more unfavorable when they are competing with the polarized particles to occupy the lowest levels. Therefore, unpaired particles tend to reside always at the bottom of the band when more pairs are polarized. With this particular spectrum topology maintained, the blocking effect is always minimized, which guarantees the survival of the strong pairing correlations when the polarization grows.

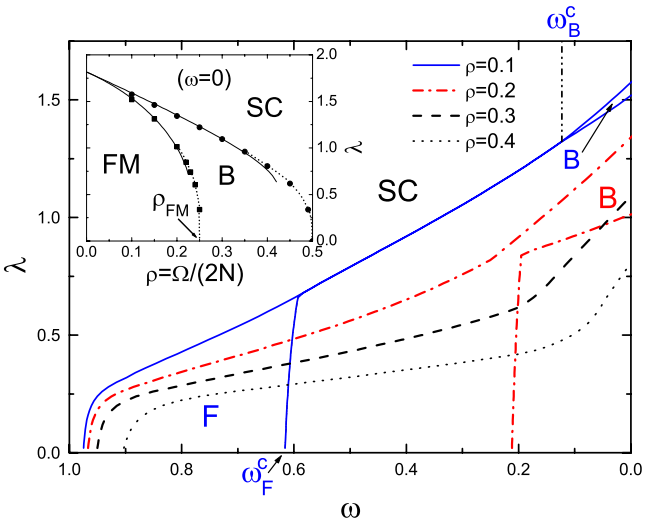


FIG. 4. (Color online) Evolution of the ground-state diagram as a function of the total density with the total number of levels $\Omega=100$. For densities $\rho=0.3$ and $\rho=0.4$, the region corresponding to the FM state shrinks to zero. At the half filling $(\rho=0.5)$ the ground state is always fully paired (SC). Inset: the ground-state diagram vs density for $\omega=0$. For comparison, we include the boundaries as obtained by means of the analytical expansion of the total energy (solid lines).

Since pairing correlations in region B remain strong after the initial polarization, one can still carry out the strong-coupling expansion in Eq. (5). The energy crossover $E_{m-1}^U+E_{m-1}^B=E_m^U+E_m^B$ determines the boundary $\omega^{m-1,m}$ that separates subregions with $m-1$ and $m$ broken pairs. This yields

$$w_+^{m-1,m} \approx \frac{\Omega-2m+2}{\Omega-4m+2}\lambda+\frac{2M-4m+2}{\Omega-4m+2}+\frac{C_1}{\lambda}, \tag{9}$$

where $C_1=\frac{(\Omega^3+\Omega^2-2M\Omega+2M^2-4\Omega-1)-(f_m+f_{m-1})}{3(\Omega-4m+2)(\Omega-2m)(\Omega-2m+2)}$ and $f_m=4m^3-m^2(6\Omega+1)+m(3\Omega^2+\Omega-4)$. One gets the corresponding asymmetry ratio via $\omega=(2-w_+)/w_+$ for the boundaries. In contrast to the slow boundary evolution in weakly correlated region F, the boundaries $\omega^{m-1,m}$ (or $w_+^{m-1,m}$) here in region B are sensitively affected by the change in the pair coupling $\lambda$, as mentioned in Sec. III A and shown in Fig. 1, providing a sign of the strong paring correlations. After the initial softened polarization at SC/B boundary, the pair breaking occurs in one-by-one steps, following $\omega^{m-1,m}>\omega^{m,m+1}$. If one reduces the pair coupling $\lambda$, these boundaries tend to converge at $\omega=\omega_B^c$. Equating $\omega^{m-1,m}=\omega^{m,m+1}$ and neglecting again the $1/\Omega$ terms, we get the same result for $\omega_B^c$ and $\lambda_B^c$ as in Eq. (8).

### D. Filling dependence of the ground-state diagram

At this point, it is interesting to investigate the evolution of the ground-state diagram for different density concentrations. The main boundaries that separate the SC and FM phases from the coexisting regions are presented in Fig. 4, showing the evolution with respect to the total density. The fully paired SC phase expands when the density approaches the half filling $(\rho=0.5)$ due to the weakening of the spin

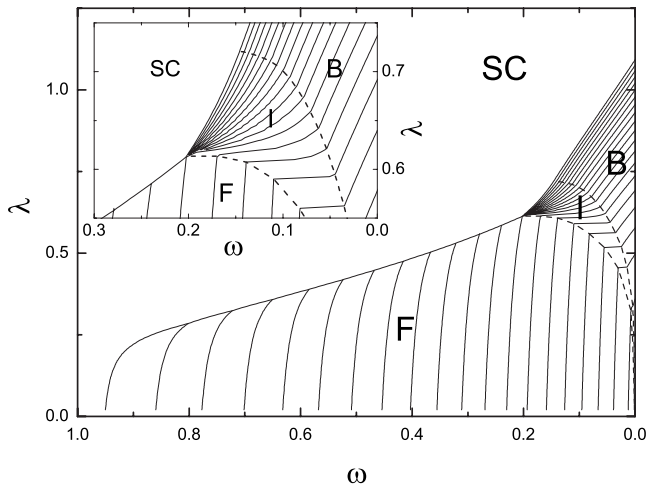


FIG. 5. Ground-state diagram as in Fig. 1 but for a total density $\rho=0.3$. Another region with the coexistence of strong pairing correlations and polarizations, region I, emerges between regions B and F. The blocked sector for states in region I is located at an intermediate position between those in states B and F. The Fermi surface in states I has a similar topology to that in states F but with a larger spectral weight in the pair density above the blocked sector.

imbalance for the uncorrelated Fermi levels. At the same time, regions F and B showing the coexistence, with weak and strong pairing correlations, respectively, expand and reduce the area of FM stability until the quarter filling $\rho \approx 0.25$ is reached, where the fully polarized phase is not stable anymore.

As marked for the case $\rho=0.1$ in Fig. 4, region B (F) exists for a bandwidth asymmetry $\omega \leq \omega_B^c$ ($\omega \geq \omega_F^c$) at low fillings. The critical asymmetry ratio $\omega_B^c$ is given by Eq. (8), while $\omega_F^c$ is approximated as

$$\omega_F^c \approx 1 - 4\rho + \frac{2(1-\lambda)(1-2\rho)}{\Omega + \lambda - 1} \tag{10}$$

by setting $m=M$ in Eq. (7) and applying the relation $\omega=(2-w_+)/w_+$. As one can see from the cases $\rho=0.1$ and $\rho=0.2$, a feature in the evolution of the coexisting phases is that regions B and F are separated at low densities but expand for a higher filling until they get connected at a certain value $\rho_{FB}$. During this process, the boundaries, $\omega_B^c$ and $\omega_F^c$, move closer to each other. Then, $\rho_{FB}$ can be extracted by equating the critical values $\omega_F^c=\omega_B^c$,

$$\rho_{FB} \approx (3-\sqrt{5})/4 = 0.19, \tag{11}$$

where we have dropped off the $1/\Omega$-order terms. As one sees in Fig. 1, the case with $\rho=0.2$ is in close proximity to such a critical point.

At higher values of the filling, another region will emerge. We notice that the variation from state F to state B at $\rho=0.3$ goes through an intermediate configuration that we have denoted by I as in Fig. 5. Such a configuration is marked by a blocked sector, with two Fermi surfaces similar to that in state F, which shifts toward the bottom of the band (but not yet reached), while the spectral distribution for the pair density presents a larger weight at energies above the blocked part than in state F. The shifting of the blocked sector away from around the uncorrelated Fermi levels gives rise to an essential difference from state F. In state F, the pair occupation above the polarized sector completely comes from the pair hopping from below. Such a pair hopping suffers from the blocking effect. However, for state I, there are some pairs above the blocked sector which do not come from the hopping of low level pairs. These pairs will still doubly occupy the levels above the blocked sector even if the pairing interaction is turned off while the same singly occupied levels are kept as in state I. Then, besides the weakened blocking effect for pairs below the blocked sector due to relatively larger values of the pair coupling λ, the pair hopping above is not hindered by the blocking effect at all. Therefore, the pairing correlations in state I are also quite strong if compared to state F.

Here, it is worth mentioning that state I has similar topology to a breach-pair state in translationally invariant and isotropic systems for which normal particles in momentum space are surrounded by superfluid.[3] While the breach-pair state is usually unstable, here the exact solution confirms that it can be the ground state in a narrow region of parameter space. Since state I possesses two Fermi surfaces, a comparison with region B exposes a Lifshitz topological transition[59] from two to one Fermi surfaces through the I/B boundary.

### E. Special limiting case: $\omega=0$

A special point in the space of parameters is the asymmetry ratio limit $\omega=0$. Such a situation is produced in the case of a bandwidth with zero amplitude for the spin minority carriers (localized levels) and a nonzero bandwidth for an itinerant spin majority component. In real systems, it corresponds to one of the possible classes of materials denoted as half-metallic.[60]

To understand the mechanisms for the coexistence in this regime, let us start with the absence of pairing. As the minority bandwidth is completely quenched ($\omega_-=0$), the single-particle energy of a full pair $\omega_+\varepsilon_+ + \omega_-\varepsilon_-$ is equal to that of a polarized particle $\omega_+\varepsilon_+$ in the spin majority band. Thus, there is no difference for the energy of the unblocked part concerning its position in the spectrum. Now let us turn on the pairing interaction. On one hand, the pair density gets reduced on a single level, due to the pair hopping over all possible unblocked levels, and as a consequence, it gets smaller than that of a singly occupied level. On the other hand, pairing correlations get stronger when the blocking effect is minimized by moving the polarized particles to the bottom of the band. Both these two mechanisms drive the ground state into a B-type configuration, for any given spin polarization, while state I or F turns out to be always less favored for any values of λ. The dependence of the phase boundaries on the density for this limiting case is presented in the inset of Fig. 4, where, as one sees, only three states (FM, SC, and B) can be realized and no F or I configuration sets in. One can get an analytic approximation for the SC/B and FM/B boundaries by setting $m=1$ and $m=M$ in Eq. (9). After neglecting the $1/\Omega$-order terms, we obtain

$$\lambda_{B,SC}^{\omega=0} \approx 1 - \rho + \sqrt{(1-\rho)^2 - 1/3},$$

$$\lambda_{\mathrm{B,FM}}^{\omega=0} \approx \frac{1-3\rho+\sqrt{(1-3\rho)^2-(1-2\rho)^2/3}}{1-2\rho},$$

respectively. These equations provide a good estimation for the boundaries in a range $\lambda > 0.75$, as shown by comparison of the solid line (analytic) and the dot line (numeric) in the inset of Fig. 4.

## IV. EFFECTS OF THE NONUNIFORMITY IN DOS ON THE COEXISTENCE OF SUPERCONDUCTIVITY AND FERROMAGNETISM

In our previous analysis, we have extensively studied the competition between superconductivity and ferromagnetism with a spin bandwidth asymmetry for a constant DOS in the single-particle spectrum. Such a hypothesis for the level distribution helps simplify the analysis in getting a physical picture to understand the competing effects between pairing correlations and spin polarizations. In this section, we turn our attention to a problem that is closer to real systems by modifying the single-particle spectrum and including the curvature effects of the particle dispersion. Our study refers to three different types of spectra that are taken from a tight-binding structure of a lattice with only the nearest-neighbor hopping in one, two, and three dimensions. The energy dependence of $\varepsilon_j$ is assumed to produce the related DOS whose spectrum is a cosine function of the momentum, $\varepsilon_{\vec{k}} \sim \Sigma_i \cos k_i$.

For a nonuniform spectrum, the pairing strength still can be described by $\lambda = g(\Omega/D)$, as $D/\Omega$ is the average value of the level spacing. As we have discussed previously, it is the competition of the level occupation between pairs and single particles that are fundamental in determining different ground-state configurations. A basic consideration shows that the variation in the DOS does not affect the leading order of the average energy per pair, $(E_g/N_\downarrow)/D = -\lambda[1-(1+P)\rho]$, as well as the competing single-particle energy $w_\sigma \varepsilon$. Therefore, it may be expected that the qualitative features of the ground-state diagram as well as the main ingredients we have extracted from the analysis for the uniform spectrum may still be valid for a nonuniform distribution. Nevertheless, it is of interest to evaluate the modifications in the ground-state diagram concerning the size of the coexisting region and the characteristics of the transition from one to another region. In this context, a special emphasis is devoted to the case of a highly inhomogeneous distribution for the energy levels. It is also worth pointing out that, while the general tendency in the variation in the DOS can be put in correspondence with the dimensionality of the system due to the dispersion under consideration, the picture may be generally applicable to other systems with a topologically affine DOS, irrespective of the lattice dimensionality.

Before considering each case separately, we give some general indications that are common to all the spectra analyzed. First, the spin-polarization mechanism arising from a spin bandwidth asymmetry can induce a fully polarized phase up to about quarter filling. Namely, above a critical density $\rho_{\mathrm{FM}} \approx 0.25$, the FM region disappears, irrespective of the features of the single-particle spectrum. In the presence of the bandwidth asymmetry, the energy difference between the opposite spins becomes smaller when particles are filled up to levels closer to the center of the band. The gain of the single-particle energy in getting polarized therefore becomes less sensitive to the asymmetry variation within the same DOS and also to the change in DOS from different spectra when the density gets closer to the half filling. Thus, the main quantitative differences for an inhomogeneous spectrum, relative to the case of uniform DOS, occur in the small density range $[0, \rho_{\mathrm{FM}}]$. Since more similarities to the uniform case exist for higher densities $\rho_{\mathrm{FM}} < \rho < 0.5$, we shall limit our attention to compare low filling cases at two typical values of the total density $\rho = 0.1$ and 0.2.

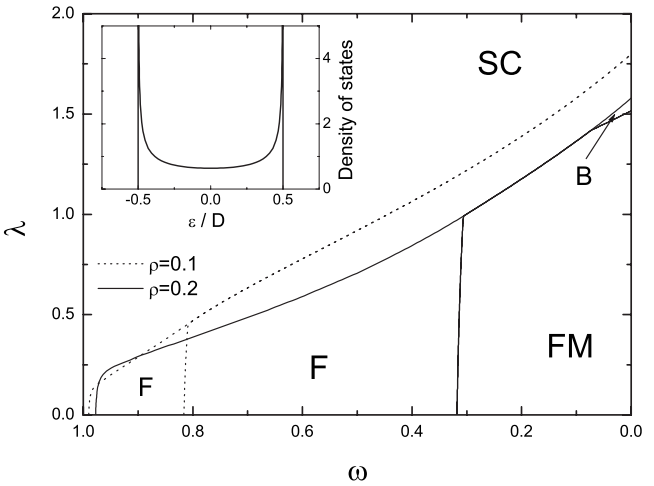


FIG. 6. Ground-state diagram for the one-dimensional spectrum $\varepsilon \sim \cos k_x$ at two values of the total density: $\rho = 0.1$ and $\rho = 0.2$. In the inset the density of states (DOS) is shown for the single-particle spectrum.

### A. One-dimensional spectrum $\epsilon \sim \cos k_x$: Weakening of the phase coexistence

We start from the one-dimensional case with a normalized dispersion $\epsilon \equiv \varepsilon/D = -\cos k_x/2$. The ground-state diagram is plotted in Fig. 6 for the main boundaries of the FM, SC, and the regions of coexistence. Compared to the case of the uniform distribution at the corresponding filling in Fig. 1, both the strongly correlated region B and the weakly correlated region F shrink at the total density $\rho = 0.2$. Region B at $\rho = 0.1$, as shown in Fig. 4, is very tiny for the homogeneous case, while now for the one-dimensional DOS, it gets completely suppressed.

To get a simple picture for the shrinking of the regions of coexistence in the ground-state diagram, we show the structure of the DOS, $\varrho(\epsilon) \equiv dn/d\epsilon = 2\Omega/(\pi\sqrt{1-4\epsilon^2})$, in the inset of Fig. 6. The DOS is very large and diverges to infinity at the band edges, while it gets quite flat near the band center. The conditions related to the modification, relative to the case of a uniform DOS, of the competition between pairing correlations and spin polarizations are different for the F and B configurations.

Indeed, the combined effect of the low fillings and the large DOS at the bottom of the spectrum makes the ferro-

magnetic configuration more favorable and the coexisting state difficult to survive. The particles at the bottom of the band have the easiest tendency to get polarized due to the large single-particle energy gain. At low fillings, most of the particles can be accommodated at the bottom of the band, thus yielding a similarly large single-particle energy gain for all the polarized particles, if the depairing occurs in region B so that the unpaired particles are located at the bottom of the band. Once it becomes favorable to polarize one pair, all the pairs can be broken at the same time due to their similar tendency toward ferromagnetism. The result is a polarization avalanche for all the pairs. Hence, in a very low filling limit $\rho=0.1$, there is no region with a coexisting state having B character. When the levels are more filled up from the bottom for a higher value of the total density as for $\rho=0.2$, there is no more space available at the bottom of the band and thus a part of the polarized pairs have to fill the levels that are higher in energy where a weaker pair-decoupling mechanism exists. Region B with the coexistence emerges in this filling range due to the softening of the spin-polarization strength, though the region of coexistence is smaller than its counterpart for the uniform spectrum. One can get similar results for the case above the half filling, since the DOS at the top of the band also goes to infinity. So, the large DOS at the edges, including the bottom and the top, of the energy band strengthens the polarization strength and thus reduces the coexistence of strong pairing correlations and polarizations.

For configurations F, unlike the states in region B, the spin-polarized pairs are removed from the Fermi level, where the DOS is much smaller than that at the bottom of the band. The polarization strength of the unpaired part is not so strong as at the bottom of the band and the pairing part dominates in the pair breaking behavior. As mentioned at the beginning of Sec. IV, the averaged leading pairing energy $(E_g/N_\downarrow)/D$ for each pair is independent of the change in the DOS. This also leads to the same initial polarization jump at the SC/F boundary as discussed in Sec. III on the uniform DOS. The formation of a polarization jump weakens not only the pairing correlations but also the polarization strength for the unpaired part, otherwise the jump would have been greater. Still, the uncorrelated Fermi level is closer to the bottom of the band, relative to the uniform DOS case, which still supports a relatively easier polarization even for the F configurations. Then, region F shrinks in comparison with the uniform case.

### B. Two- and three-dimensional spectra: The enhanced coexistence of superconductivity and ferromagnetism

The analysis in the one-dimensional case shows that a large DOS at the band edges makes it difficult to compromise for the strong pairing correlations and the asymmetric bandwidth induced polarizations at low fillings. Then we speculate that a small DOS at the edges will enhance the coexistence of superconductivity and ferromagnetism. We find that this is indeed the case for the two-dimensional and three-dimensional spectra. In fact, for both spectra, less level distributions occur at the edges of the band than near the center, while the area of the regions for the coexistence of pairing correlations and polarizations is greatly broadened.

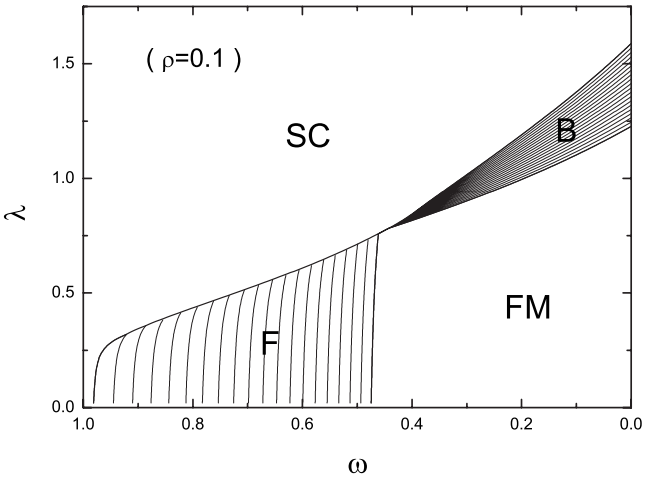


FIG. 7. Ground-state diagram for the two-dimensional spectrum $\varepsilon \sim \cos k_x + \cos k_y$ at a given total density $\rho=0.1$ for the total number of levels $\Omega=200$.

#### *1. Ground-state diagram for the two-dimensional spectrum*

A normalized two-dimensional single-particle dispersion, given by $\epsilon=-(\cos k_x+\cos k_y)/4$, yields a DOS,

$$\frac{dn}{d\epsilon} = \Omega \int_0^{\arccos(4|\epsilon|-1)} \frac{1/\pi^2}{\sqrt{1-[4|\epsilon|-\cos(k_x)]^2}} dk_x.$$

The number of states below a given energy $\varepsilon$ is proportional to the area in the two-dimensional momentum plane, where all states with the single-particle energy below $\varepsilon$ are included. One can readily obtain the above DOS expression by examining the change in this area if a small increase in $\varepsilon$ is given. We plot the DOS profile in Fig. 8(c). The detailed ground-state diagrams are presented in Figs. 7 and 8 for fillings $\rho=0.1$ and $\rho=0.2$, respectively, assuming a total number of 200 levels. Compared with the uniform case, the region size of the polarization-pairing coexistence is enlarged both for regions F and B. Moreover, the diagram in Fig. 8 has a broader F/B connection. A narrow region I now emerges between regions B and F due to the wider connection between them.

Let us consider region B. From the analysis of the one-dimensional case, it is now easy to understand the reason for the enhancement of the coexistence. Here, for the two-dimensional case, the DOS is smaller at the band edges while it becomes larger for the energy levels close to the center of the band. Such a tendency of the DOS variation is opposite to the coexistence weakening in the one-dimensional case. Then, despite of a strong polarization tendency at the band edges, the bottom of the band with a smaller DOS has less space to accommodate the polarized pairs. Filling up the spectrum to higher levels reduces the magnetic energy gain in polarizations. Thus, it requires a larger band asymmetry to compensate the softening of the spin-polarization strength in reaching the same magnetization amplitude as in the case of the uniform spectrum. Such a condition leads to a wider range of $\omega$ for the coexistence. In other words, the softening

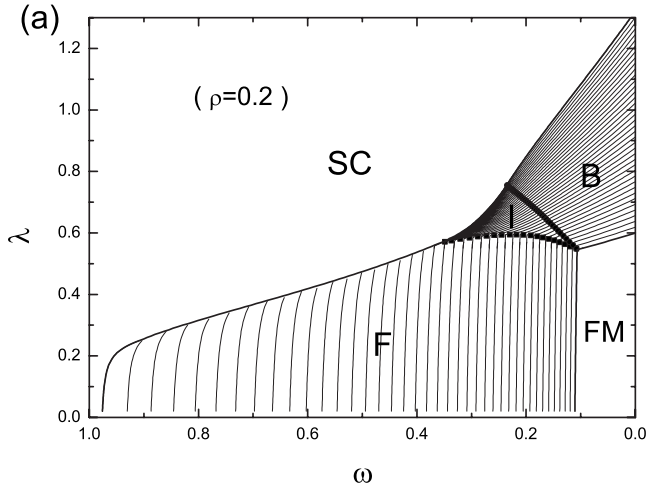


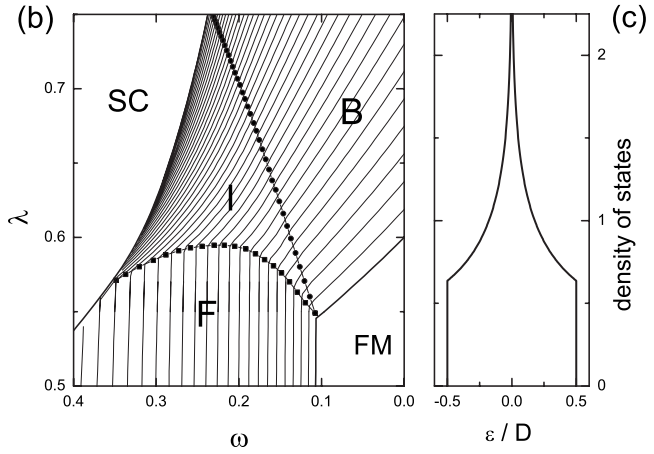


FIG. 8. (a) Ground-state diagram for the two-dimensional spectrum $\varepsilon \sim \cos k_x + \cos k_y$ at a given total density $\rho = 0.2$ for the total number of levels $\Omega = 200$. Region I emerges between regions F and B. (b) A zoomed view of panel (a) for regions F, I, and B. (c) The DOS for the single-particle spectrum.

of the spin-polarization mechanism makes it easier for polarized particles and strongly correlated pairs to coexist.

#### *2. Ground-state diagram for the three-dimensional spectrum*

We turn to a system with a normalized three-dimensional band $\epsilon = -(\cos k_x + \cos k_y + \cos k_z)/6$. At a filling $\rho = 0.1$, the coexisting regions F and B are of greater sizes if compared to the two-dimensional case; now they are even connected via the intermediate region I (see Fig. 9). In the case $\rho = 0.2$, the coexisting regions are also more stable in comparison with the uniform DOS case. When compared to the two-dimensional case, a new distinct feature for the three-dimensional case is observed: region B is separated into two subregions B1 and B2, with relatively sparser and denser boundaries, respectively. The same happens for region I, as in the subregions I1 and I2. The subregions exhibit different slopes in the magnetization, as shown by Fig. 10(c).

The DOS for the three-dimensional case takes the form

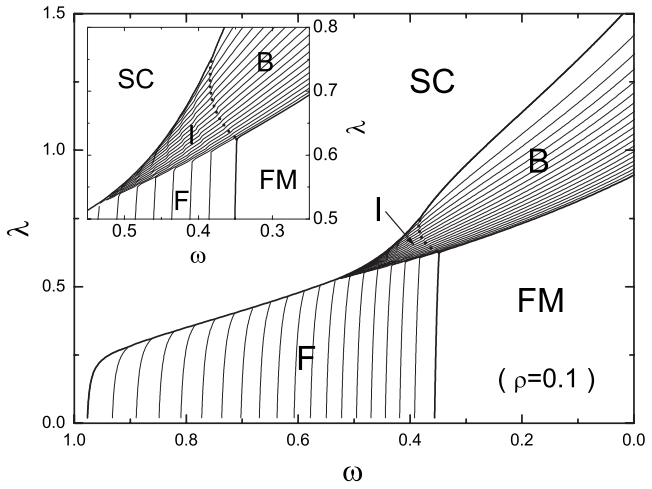


FIG. 9. Ground-state diagram for three-dimensional spectrum $\varepsilon \sim \cos k_x + \cos k_y + \cos k_z$ at a given total density $\rho = 0.1$ for the total number of levels $\Omega = 200$.

$$\frac{dn}{d\epsilon} = 6\Omega \int_0^{2\pi} \int_0^{2\pi} \frac{dk_x dk_y/(2\pi)^3}{\sqrt{1-(6\epsilon+\cos k_x+\cos k_y)^2}},$$

which is shown in Fig. 10(d). Going from the edges to the center of the band, the DOS increases quickly from zero and then suddenly turns to be flat. As discussed for the two-dimensional case, a small DOS amplitude at band edges strengthens the coexistence of pairing correlations and polarizations. This scenario is even better realized when at the bottom of the band the DOS is suppressed to zero in the three-dimensional case (for the two-dimensional case the DOS at the band edge is still finite). Therefore, for a low density $\rho = 0.1$, region B is highly enhanced. For a higher filling $\rho = 0.2$, the increase in the spin polarization leads to the level occupations in the flat DOS zone. In the range of such a uniform DOS, the tendency to the coexistence is not so strong as at low polarizations, thus leading to a subregion B2 similar to that in the uniform DOS case. The changeover from a rapidly varying DOS to a flat one results in different behaviors inside the coexisting regions. Since the coexistence in subregion B1 is more robust than in subregion B2, it tends to broaden the size of region with the coexistence. Then, boundaries in regions B1 turn out to be sparser than those in subregion B2 because wider boundary spacing yields a broader region size for the coexistence. This results in the unequal rises of the magnetization in the two subregions [see Fig. 10(c)]. A similar analysis also applies for the subregions I1 and I2.

Region F is not much affected by the DOS structure. Although the DOS is large for the two-dimensional case close to the center of the band or has obvious curvature changeover in the three-dimensional case, the strength for breaking pairs does not change much due to the insensitive response of the unpaired energy to the bandwidth asymmetry for levels close to the center of the band. Moreover, the initial jump of polarizations minimizes both the pairing correlations and the polarization strength, as also mentioned in the one-dimensional case. Hence, the behavior of the pair breaking in

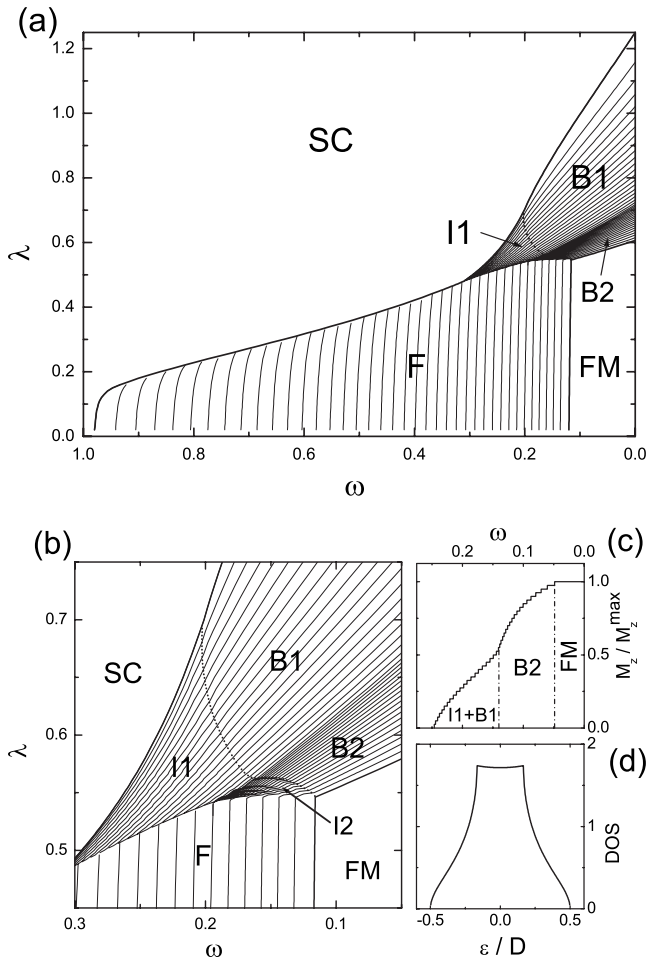


FIG. 10. (a) Ground-state diagram for the three-dimensional spectrum $\varepsilon \sim \cos k_x + \cos k_y + \cos k_z$ at $\rho = 0.2$ for the total number of levels $\Omega = 200$. The variation in the magnetization in regions I and B exhibits two different subregions that are indicated as I1, I2 and B1, B2, respectively. (b) A zoomed view of the panel (a) with a focus on the area where regions F, I, and B get connected. (c) An example of evolution for the magnetization $M_z$ versus the bandwidth asymmetry at a pair coupling $\lambda = 0.58$. The band asymmetry goes through the I1, B1, B2, and FM regions, showing a changeover at B1/B2 boundary. (d) Representation of the DOS for the three-dimensional spectrum.

region F is quite similar to the uniform DOS case, except for some expansion in the region size.

## V. CONCLUSIONS

In conclusion, we have exactly solved an extended version of the reduced BCS model for particles that get paired in the presence of a polarization arising from spin dependent bandwidths. The evolution of the ground-state diagram has been discussed in the full parameter space of the pair coupling and the bandwidth asymmetry as a function of filling for different types of spectrum topologies. Compared to previous studies, the results indicate the possibility for a coexisting state of strong pairing correlations and finite spin polarizations. We point out that our analysis has been performed within a general framework, which is intended not only for bulk type but also for nanoscopic or mesoscopic systems where the size may play a relevant role. The first main outcome of the present investigation is the realization of a strongly paired configurations with partial polarizations, i.e., states B as well as states I, via a combination of filling control and variation in relative pair coupling strength in the presence of a strong bandwidth asymmetry. Practically, the pair coupling strength may be varied either by choosing proper materials or by changing the sample size.[36] Furthermore, by investigating different single-particle spectra, we have analyzed the influence of nonuniformity in the DOS on the coexistence of strong pairing correlations and finite polarizations. Depending on the curvature and the amplitude of the DOS, it is possible to understand the proper conditions under which the coexistence of superconductivity and itinerant ferromagnetism may be enhanced. Indeed, we have shown that a large value of the DOS at the edges of the band is in general detrimental to the coexistence induced by the bandwidth asymmetry. Otherwise, for a band spectrum with a lower (or zero) amplitude of the DOS at energies close to the edges, the region where strong pairing correlations and spin polarizations coexist in the ground state is significantly enhanced.

As concluding remarks, we underline that, while our results do not correspond to specific available experimental data, there are material systems that may be directly connected to the model Hamiltonian used in our analysis. As extensively discussed throughout the paper, the key points of our study concern the realization of spin-polarized superconducting states with strong pair correlations induced from the spin-split bandwidths (effective masses) and the suitable topology of the density of states. These elements can be used to connect our investigation with some observations related to specific material systems. Indeed, the observation of spin dependent masses induced by a magnetic field in heavy-fermion superconductors as $CeCoIn_5$ (Ref. 61) and $CePd_2Si_2$ (Ref. 62) makes these materials potential candidates to match the microscopic conditions of the examined model Hamiltonian. Here, the spin dependence of the quasiparticle mass is induced by the applied magnetic field and arises from the interplay between strong electron correlations and spin polarization as discussed within different theoretical approaches.[63–65] Of particular interest for our study is $CeCoIn_5$. Specific heat measurements revealed a second-order phase-transition line within the superconducting state, providing evidence for a superconducting phase at the high-field-low-temperature side of the phase diagram[66,67] where the amplitude of the spin-split masses is significant. Experimental indications point toward the realization of a FFLO state in this range of field and temperature even if several unexpected features have been detected as, for example, the remarkable dependence on the magnetic field and temperature of the phase boundary between the putative FFLO and non-FFLO states.[16] Since it has been shown that the applied field modifies the ratio of the spin dependent effective masses, we speculate that state B or I obtained in our analysis of the ground-state diagram, with a second-order transition at SC-B or SC-I boundary, can be considered for the phase found in the field-temperature phase diagram of the $CeCoIn_5$.

Other cases, in which our analysis can find application, refer to hybrid systems like heterostructures made of junctions with interfaced superconductors and half-metallic materials as for $NbTiN/CrO_2/NbTiN$ samples.[68] Here, a giant proximity effect is observed by detecting a supercurrent flowing through the half-metal even if the size of the $CrO_2$ is much larger than the expected proximity leaking distance. Our analysis indicates that the coexistence of strong pair correlations and ferromagnetism is indeed favored in proximity of the half-metallic limit, where one type of spin carrier gets insulating (zero bandwidth) and the other one is metallic. Thus, the configurations that are stable in this part of the phase diagram may play a role at the interface between a singlet-type superconductor and a half-metal ferromagnet, which in turn influences the proximity effect through the way the pairs adapt themselves within the half-metallic electron liquid.

## ACKNOWLEDGMENTS

This work is partially supported by the National Natural Science Foundation of China (Grant No. 10774197) and the Natural Science Foundation of Chongqing (Grant No. CSTC2008BC2023).

[1] A. I. Buzdin, Rev. Mod. Phys. **77**, 935 (2005); F. S. Bergeret, A. F. Volkov, and K. B. Efetov, *ibid.* **77**, 1321 (2005).
[2] R. Casalbuoni and G. Nardulli, Rev. Mod. Phys. **76**, 263 (2004).
[3] W. V. Liu and F. Wilczek, Phys. Rev. Lett. **90**, 047002 (2003); Michael McNeil Forbes, E. Gubankova, W. V. Liu, and F. Wilczek, *ibid.* **94**, 017001 (2005).
[4] A. Sedrakian and U. Lombardo, Phys. Rev. Lett. **84**, 602 (2000).
[5] S. Giorgini, L. P. Pitaevskii, and S. Stringari, arXiv:0706.3360, Rev. Mod. Phys. (to be published), and references therein.
[6] A. A. Abrikosov and L. P. Gorkov, Zh. Eksp. Teor. Fiz. **39**, 1781 (1960) [Sov. Phys. JETP **12**, 1243 (1961)].
[7] B. T. Matthias, H. Suhl, and E. Corenzwit, Phys. Rev. Lett. **1**, 449 (1958).
[8] See, for example, *Superconductivity in Ternary Compounds*, edited by M. B. Maple and F. Fisher (Springer-Verlag, Berlin, 1982).
[9] P. W. Anderson and H. Suhl, Phys. Rev. **116**, 898 (1959).
[10] E. I. Blount and C. M. Varma, Phys. Rev. Lett. **42**, 1079 (1979).
[11] A. M. Clogston, Phys. Rev. Lett. **9**, 266 (1962).
[12] B. S. Chandrasekhar, Appl. Phys. Lett. **1**, 7 (1962).
[13] A. I. Larkin and Yu. N. Ovchinnikov, Zh. Eksp. Teor. Fiz. **47**, 1136 (1964) [Sov. Phys. JETP **20**, 762 (1975)].
[14] P. Fulde and R. A. Ferrell, Phys. Rev. **135**, A550 (1964).
[15] C. Petrovic, P. G. Pagliuso, M. F. Hundley, R. Movshovich, J. L. Sarrao, J. D. Thompson, Z. Fisk, and P. Monthoux, J. Phys.: Condens. Matter **13**, L337 (2001).
[16] K. Kumagai, M. Saitoh, T. Oyaizu, Y. Furukawa, S. Takashima, M. Nohara, H. Takagi, and Y. Matsuda, Phys. Rev. Lett. **97**, 227002 (2006).
[17] T. Mizushima, K. Machida, and M. Ichioka, Phys. Rev. Lett. **94**, 060404 (2005).
[18] J. Kinnunen, L. M. Jensen, and P. Torma, Phys. Rev. Lett. **96**, 110403 (2006).
[19] K. Yang, *Pairing in Fermionic Systems: Basic Concepts and Modern Applications*, Mark Alford, John Clark, and Armen Sedrakian, (World Scientific, 2006), p. 253–268.
[20] See *Ruthenate and Rutheno-Cuprate Materials: Unconventional Superconductivity, Magnetism and Quantum Phase Transitions*, Springer Lecture Notes in Physics Vol. 603, edited by C. Noce, A. Vecchione, M. Cuoco, and A. Romano (Springer-Verlag, Berlin, 2002), p. 303.
[21] D. Fay and J. Appel, Phys. Rev. B **22**, 3173 (1980).
[22] S. S. Saxena, P. Agarwal, K. Ahilan, F. M. Grosche, R. K. W. Haselwimmer, M. J. Steiner, E. Pugh, I. R. Walker, S. R. Julian, P. Monthoux, G. G. Lonzarich, A. Huxley, I. Sheikin, D. Braithwaite, and J. Flouquet, Nature (London) **406**, 587 (2000).
[23] D. Aoki, A. Huxley, E. Ressouche, D. Braithwaite, J. Flouquet, J.-P. Brison, E. Lhotel, and C. Paulsen, Nature (London) **413**, 613 (2001).
[24] C. Pfleiderer, M. Uhlarz, S. M. Hayden, R. Vollmer, H. v. Lohneysen, N. R. Bernhoeft, and G. G. Lonzarich, Nature (London) **412**, 58 (2001).
[25] N. T. Huy, A. Gasparini, D. E. de Nijs, Y. Huang, J. C. P. Klaasse, T. Gortenmulder, A. de Visser, A. Hamann, T. Gorlach, and H. v. Lohneysen, Phys. Rev. Lett. **99**, 067006 (2007).
[26] E. A. Yelland, S. M. Hayden, S. J. C. Yates, C. Pfleiderer, M. Uhlarz, R. Vollmer, H. v. Lohneysen, N. R. Bernhoeft, R. P. Smith, S. S. Saxena, and N. Kimura, Phys. Rev. B **72**, 214523 (2005).
[27] F. Levy, I. Sheikinm, and A. Huxley, Nat. Phys. **3**, 460 (2007).
[28] G. G. Lonzarich, Nat. Phys. **3**, 453 (2007).
[29] N. I. Karchev, K. B. Blagoev, K. S. Bedell, and P. B. Littlewood, Phys. Rev. Lett. **86**, 846 (2001).
[30] Y. Zhou, J. Li, and C. D. Gong, Phys. Rev. Lett. **91**, 069701 (2003).
[31] R. Shen, Z. M. Zheng, and D. Y. Xing, Phys. Rev. Lett. **91**, 069702 (2003); R. Shen, Z. M. Zheng, S. Liu, and D. Y. Xing, Phys. Rev. B **67**, 024514 (2003).
[32] Y. N. Joglekar and A. H. MacDonald, Phys. Rev. Lett. **92**, 199705 (2004).
[33] K. B. Blagoev, K. S. Bedell, and P. B. Littlewood, Phys. Rev. Lett. **92**, 199706 (2004).
[34] Z.-J. Ying, M. Cuoco, C. Noce, and H.-Q. Zhou, Phys. Rev. B **74**, 012503 (2006).
[35] Z.-J. Ying, M. Cuoco, C. Noce, and H.-Q. Zhou, Phys. Rev. B **74**, 214506 (2006).
[36] Z.-J. Ying, M. Cuoco, C. Noce, and H.-Q. Zhou, Phys. Rev. B **76**, 132509 (2007).
[37] I. L. Kurland, I. L. Aleiner, and B. L. Altshuler, Phys. Rev. B **62**, 14886 (2000).
[38] I. L. Aleiner, P. W. Brouwer, and L. I. Glazman, Phys. Rep. **358**, 309 (2002).
[39] S. Schmidt, Y. Alhassid, and K. Van Houcke, Europhys. Lett. **80**, 47004 (2007).
[40] G. Falci, R. Fazio, and A. Mastellone, Phys. Rev. B **67**, 132501 (2003).

[41] W.-H. Li, C.-W. Wang, C.-Y. Li, C. K. Hsu, C. C. Yang, and C.-M. Wu, Phys. Rev. B **77**, 094508 (2008).
[42] M. Cuoco, P. Gentile, and C. Noce, Phys. Rev. Lett. **91**, 197003 (2003).
[43] R. W. Richardson, Phys. Rev. **141**, 949 (1966); J. Math. Phys. **18**, 1802 (1977).
[44] J. von Delft and D. C. Ralph, Phys. Rep. **345**, 61 (2001), and references therein.
[45] J. Dukelsky, S. Pittel, and G. Sierra, Rev. Mod. Phys. **76**, 643 (2004), and references therein.
[46] Z.-J. Ying, M. Cuoco, C. Noce, and H.-Q. Zhou, Phys. Rev. Lett. **100**, 140406 (2008).
[47] J. E. Hirsch, Phys. Rev. B **40**, 2354 (1989); **40**, 9061 (1989); **59**, 6256 (1999).
[48] C. Zener, Phys. Rev. **82**, 403 (1951).
[49] P. W. Anderson and H. Hasegawa, Phys. Rev. **100**, 675 (1955).
[50] P. F. Bedaque, H. Caldas, and G. Rupak, Phys. Rev. Lett. **91**, 247002 (2003).
[51] G.-D. Lin, W. Yi, and L.-M. Duan, Phys. Rev. A **74**, 031604(R) (2006); W.-C. Su, *ibid.* **74**, 063627 (2006); C.-H. Pao, Shin-Tza Wu, and S.-K. Yip, *ibid.* **76**, 053621 (2007).
[52] M. Iskin and C. A. R. Sá de Melo, Phys. Rev. Lett. **97**, 100404 (2006); M. M. Parish, F. M. Marchetti, A. Lamacraft, and B. D. Simons, *ibid.* **98**, 160402 (2007).
[53] H.-Q. Zhou, J. Links, R. H. McKenzie, and M. D. Gould, Phys. Rev. B **65**, 060502(R) (2002).
[54] E. A. Yuzbashyan, A. A. Baytin, and B. L. Altshuler, Phys. Rev. B **68**, 214509 (2003).
[55] J. M. Dickey and A. Paskin, Phys. Rev. B **1**, 851 (1970).
[56] M. Strongin, R. S. Thompson, O. F. Kammerer, and J. E. Crow, Phys. Rev. B **1**, 1078 (1970).
[57] W.-H. Li, C. C. Yang, F. C. Tsao, S. Y. Wu, P. J. Huang, M. K. Chung, and Y. D. Yao, Phys. Rev. B **72**, 214516 (2005).
[58] M. Schechter, Y. Imry, Y. Levinson, and J. von Delft, Phys. Rev. B **63**, 214518 (2001).
[59] I. M. Lifshitz, Zh. Eksp. Teor. Fiz. **38**, 1569 (1960) [Sov. Phys. JETP **11**, 1130 (1960)].
[60] J. M. D. Coey and M. Venkatesan, J. Appl. Phys. **91**, 8345 (2002).
[61] A. McCollam, S. R. Julian, P. M. C. Rourke, D. Aoki, and J. Flouquet, Phys. Rev. Lett. **94**, 186401 (2005).
[62] I. Sheikin, A. Groger, S. Raymond, D. Jaccard, D. Aoki, H. Harima, and J. Flouquet, Phys. Rev. B **67**, 094420 (2003).
[63] P. Korbel, J. Spalek, W. Wojcik, and M. Acquarone, Phys. Rev. B **52**, R2213 (1995).
[64] K. Held, M. Ulmke, N. Blumer, and D. Vollhardt, Phys. Rev. B **56**, 14469 (1997).
[65] S. Onari, H. Kontani, and Y. Tanaka, J. Phys. Soc. Jpn. **77**, 023703 (2008).
[66] H. A. Radovan, N. A. Fortune, T. P. Murphy, S. T. Hannahs, E. C. Palm, S. W. Tozer, and D. Hall, Nature (London) **425**, 51 (2003).
[67] A. Bianchi, R. Movshovich, C. Capan, P. G. Pagliuso, and J. L. Sarrao, Phys. Rev. Lett. **91**, 187004 (2003).
[68] R. S. Keizer, S. T. B. Goennenwein, T. M. Klapwijk, G. Miao, G. Xiao, and A. Gupta, Nature (London) **439**, 825 (2006).